Morphological Evolution of Self-Assembled Polyaniline Nanostuctures Obtained by pH-stat Chemical Oxidation

Cosmin Laslau,[†] Zoran D. Zujovic,[†] Lijuan Zhang,[†] Graham A. Bowmaker,[†] and Jadranka Travas-Sejdic*[,†,‡]

Polymer Electronics Research Centre, Department of Chemistry, University of Auckland, Private Bag 92019, Auckland, New Zealand, and MacDiarmid Institute for Advanced Materials and Nanotechnology, PO Box 600, Wellington, New Zealand

Received December 21, 2008

The chemical oxidation of polyaniline is carried out at constant acidity, investigating six separate pH levels (pH = 1, 2, 3, 4, 5, and 6). All prior studies on polyaniline self-assembly used a falling-pH or a temporarily buffered falling-pH method, making this the first application of pH-stat techniques to the study of polymer nanostructure formation. This allows us to isolate with improved precision the various nanostructures formed at different stages of polyaniline self-assembly, which include spheres, flakes and ribbons at neutral pH, fibers and tubes at mildly acidic pH, and grains at highly acidic pH. The evolution of these structures is investigated as a function of both pH and time. This approach results in the observation of two previously unnoticed phenomena: the morphology is found to evolve as a function of time even when pH is kept constant, and polyaniline nanotubes are formed at a constant acidity. Both of these results have important implications for existing self-assembly theories. Fourier transform infrared spectroscopy is used to investigate the polyaniline compositional and structural evolution underlying the visible morphological changes and shows that as pH falls there is increased protonation, decreased ortho-coupling, lower phenazine presence, and less sulfonation. The time evolution, on the other hand, shows increased sulfonation and decreased oxidation. Ultraviolet−visible spectroscopy shows a mixture of delocalized and localized polaron behavior for the pH-1-stat to pH-3-stat products, and insulating characteristics for the higher pH structures. This is confirmed by four-point conductivity measurements.

1. Introduction

Conducting polymer nanostructures combine three important advantages: first, the ubiquity of synthetic polymers, which are used in larger quantities than any other type of material in the world;[1] second, the unique ability of conducting polymers to achieve the high conductivity of a metal while maintaining the malleable processing advantages of a plastic;[2] and third, the high surface area,[3] improved strength,[4] and unique behavior that can be gained as dimensions are scaled down to approximately 100 nm or lower.[5] Having all these properties in one material can lead to exciting applications in chemical and biological sensors, coatings, field emission displays, actuators, photovoltaic cells, and transistors.[6]

This study focuses on polyaniline (PANI), a conducting polymer unique for its reversible and relatively simple acid−base doping−dedoping pathway, useful for tuning the electrical and optical properties of the material.[7] It also exhibits high conductivity, excellent environmental stability, and is straightforward to synthesize.[8] PANI nanostructures are typically formed using electrospinning, templates, or self-assembly,[9] with each method having its advantages and drawbacks. Template assisted synthesis can achieve excellent uniformity because of its PANI-molding channels or pores but cannot readily be scaled up for mass production.[10] This contrasts with self-assembly, which is theoretically well-suited for high volume production but has poor uniformity and depends on added structurally directing functional molecules. The goal of this paper is to help address these PANI self-assembly issues of uniformity and repeatability, by using pH-stat methods to map the variety of nanostructure types that form during the individual stages of synthesis. This in turn should assist in gaining a better understanding of the mechanism of PANI nanotube formation.

The variety of PANI nanostructures produced by self-assembly has been well-documented, with reports ranging from the typical fibers,[11] tubes,[12] and particles[13] to more

* Corresponding author. E-mail: j.travas-sejdic@auckland.ac.nz.
† University of Auckland.
‡ MacDiarmid Institute for Advanced Materials and Nanotechnology.

(1) Heeger, A. J. *Synth. Met.* **2002**, *125*, 23.
(2) Shirakawa, H.; Louis, E. J.; MacDiarmid, A. G.; Chiang, C. K.; Heeger, A. J. *J. Chem. Soc., Chem. Commun.* **1977**, *177*, 578.
(3) Rolison, D. R. *Science* **2003**, *299*, 1698.
(4) Wong, E. W.; Sheehan, P. E.; Lieber, C. M. *Science* **1997**, *277*, 1971.
(5) Alivisatos, A. P. *Science* **1996**, *271*, 933.
(6) Jang, J. *Adv. Polym. Sci.* **2006**, *199*, 189.
(7) Li, G.; Zhang, C.; Peng, H. *Macromol. Rapid Commun.* **2007**, *29*, 63.
(8) Li, D.; Kaner, R. B. *J. Am. Chem. Soc.* **2006**, *128*, 968.
(9) Skotheim, T. A. Reynolds, J. R. *Conjugated Polymers: Theory, Synthesis, Properties, and Characterization*, 3rd ed.; CRC Press: Boca Raton, 2006.
(10) Wan, M. *Adv. Mater.* **2008**, *20*, 2926.
(11) Huang, J.; Virji, S.; Weiller, B. H.; Kaner, R. B. *J. Am. Chem. Soc.* **2003**, *125*, 314.
(12) Qiu, H.; Wan, M.; Matthews, B.; Dai, L. *Macromolecules* **2001**, *34*, 675.
(13) Stejskal, J.; Sapurina, I. *J. Colloid Interface Sci.* **2004**, *274*, 489.

10.1021/cm803447a CCC: $40.75
Published on Web 02/11/2009

exotic leafs,[14] cubes,[15] rods,[16] spheres,[17] flakes,[18] disks,[7] "brains",[19] and sheets.[20] Attempts to understand and improve these nanostructures are complicated by poorly controlled size distributions[21] and surface texture variance,[22] as well as a lack of homogeneity: nanofibers, nanotubes, nanoparticles, nanoflakes, and nanospheres are often seen mixed together as a final product.[23−25] So far the best-developed formation theories have been two competing models that aim to describe tubular self-assembly, with one proposing the importance of micelle aggregation[10,26−34] and the other focusing on the presence of a phenazine backbone.[20,23,25,35,36] However, a well defined theory that encompasses the full nanostructure spectrum remains elusive, with discussions often deferring to molecular interaction catch-alls such as hydrogen bonding, van der Waals forces, and $\pi-\pi$ stacking.[33] Progress is made difficult by the myriad of factors that can influence the self-assembly of PANI, including concentration ratios,[27] temperature,[22] solvents,[37] surfactants,[38] acids,[34] oxidants,[26] and pH.[17] Studies have looked to selectively account for one or several of these effects, thus shedding light on individual facets of what may be a larger self-assembly framework.

This paper will focus on the effect of pH on the formation of nanostructures during the oxidative polymerization of aniline, as illustrated in Scheme 1. It has been widely reported that during the self-assembly of PANI nanostructures the pH value of the solution falls,[10,17,18,20,22−26,30,33,39−46] typically from pH 7 to pH 1 (see Figure 1). The reason for this change in acidity is the generation of protons during the oxidation of aniline.[20]

Scheme 1. Reaction for the Oxidative Polymerization of Aniline, with Ammonium Persulfate as the Oxidant[a]

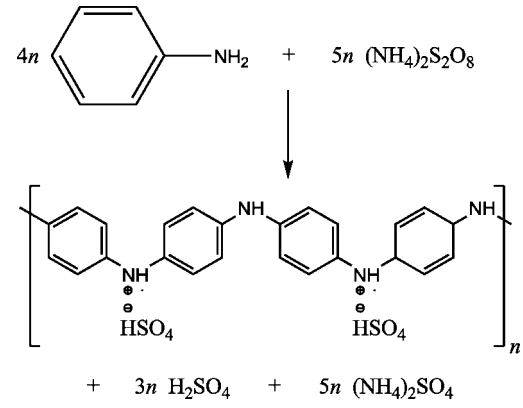

[a] Adapted from Trchova et al.[20]

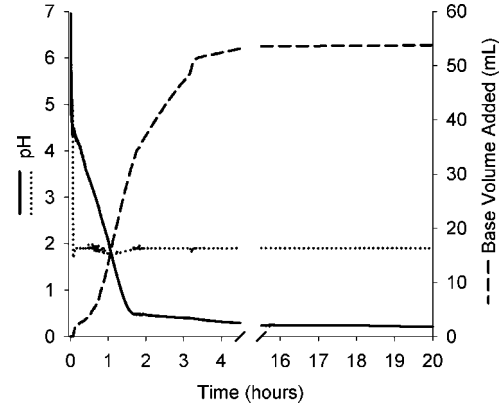

Figure 1. Solid line shows the typical falling-pH profile of "normal" PANI nanotube synthesis. The dotted line shows the pH−2-stat synthesis profile, and the dashed line shows the necessary volume added to keep the pH constant.

In studying the effects of constant acidity, we are building upon a previous report from our group, where the pH was temporarily buffered for approximately 3 h.[18] The key difference is that the present study holds the pH at the same value during the entire 20 h reaction, which to the best of our knowledge is the first application of pH-stat techniques to study the self-assembly of polymer nanostructures. (pH-stat polymer studies were previously carried out by Minami et al., but their scope was to model the reaction kinetics of 3,5-xylidine[47] and to produce polystyrene/PANI core/shell composites.[48])

(14) Han, J.; Song, G.; Guo, R. *Adv. Mater.* **2007**, *19*, 2993.
(15) Zhu, Y.; Li, J.; Wan, M.; Jiang, L. *Polymer* **2008**, *49*, 3419.
(16) Jang, J.; Bae, J.; Lee, K. *Polymer* **2005**, *46*, 3677.
(17) Stejskal, J.; Sapurina, I.; Trchova, M.; Konyushenko, E. N. *Macromolecules* **2008**, *41*, 3530.
(18) Zhang, L.; Zujovic, Z. D.; Peng, H.; Bowmaker, G. A.; Kilmartin, P. A.; Travas-Sejdic, J. *Macromolecules* **2008**, *41*, 8877.
(19) Zhu, Y.; Li, J.; Wan, M.; Jiang, L.; Wei, Y. *Macromol. Rapid Commun.* **2007**, *28*, 1339.
(20) Trchova, M.; Sedenkova, I.; Konyushenko, E. N.; Stejskal, J.; Holler, P.; Ciric-Marjanovic, G. *J. Phys. Chem. B* **2006**, *110*, 9461.
(21) Langer, J. J.; Framski, G.; Golczak, S. *Synth. Met.* **2001**, *121*, 1319.
(22) Stejskal, J.; Spirkova, M.; Riede, A.; Helmstedt, M.; Mokrevac, P.; Prokes, J. *Polymer* **1999**, *40*, 2487.
(23) Janosevic, A.; Ciric-Marjanovic, G.; Marjanovic, B.; Holler, P.; Trchova, M.; Stejskal, J. *Nanotechnology* **2008**, *19*, 135606.
(24) Konyushenko, E. N.; Stejskal, J.; Sedenkova, I.; Trchova, M.; Sapurina, I.; Cieslar, M.; Prokes, J. *Polym. Int.* **2006**, *55*, 31.
(25) Stejskal, J.; Sapurina, I.; Trchova, M.; Konyushenko, E. N.; Holler, P. *Polymer* **2006**, *47*, 8253.
(26) Ding, H.; Wan, M.; Wei, Y. *Adv. Mater.* **2007**, *19*, 465.
(27) Zhang, L.; Wan, M. *Adv. Funct. Mater.* **2003**, *13*, 815.
(28) Wan, M.; Wei, Z.; Zhang, Z.; Zhang, L.; Huang, K.; Yang, Y. *Synth. Met.* **2003**, *135−136*, 175.
(29) Zhang, Z.; Wei, Z.; Wan, M. *Macromolecules* **2002**, *35*, 5937.
(30) Zhang, L.; Zhang, L.; Wan, M. *Eur. Polym. J.* **2008**, *44*, 2040.
(31) Wei, Z.; Zhang, Z.; Wan, M. *Langmuir* **2002**, *18*, 917.
(32) Long, Y.; Chen, Z.; Wang, N.; Ma, Y.; Zhang, Z.; Zhang, L.; Wan, M. *Appl. Phys. Lett.* **2003**, *83*, 1863.
(33) Ding, H.; Shen, J.; Wan, M.; Chen, Z. *Macromol. Chem. Phys.* **2008**, *209*, 864.
(34) Zhang, L.; Long, Y.; Chen, Z.; Wan, M. *Adv. Funct. Mater.* **2004**, *14*, 693.
(35) Ciric-Marjanovic, G.; Trchova, M.; Stejskal, J. *Int. J. Quantum Chem.* **2008**, *108*, 318.
(36) Ciric-Marjanovic, G.; Konyushenko, E. N.; Trchova, M.; Stejskal, J. *Synth. Met.* **2008**, *158*, 200.
(37) Huang, J.; Kaner, R. B. *Chem. Commun.* **2006**, *4*, 367.
(38) Stejskal, J.; Omastova, M.; Fedorova, S.; Prokes, J.; Trchova, M. *Polymer* **2003**, *44*, 1353.
(39) Zhang, Z.; Wang, L.; Deng, J.; Wan, M. *React. Funct. Polym.* **2008**, *68*, 1081.
(40) Chiou, N.-R.; Lee, L. J.; Epstein, A. J. *Chem. Mater.* **2007**, *19*, 3589.
(41) Zhou, C.; Han, J.; Song, G.; Guo, R. *Eur. Polym. J.* **2008**, *44*, 2850.
(42) Zhong, W.; Wang, Y.; Yan, Y.; Sun, Y.; Deng, J.; Yang, W. *J. Phys. Chem. B* **2007**, *111*, 3918.
(43) Jin, E.; Liu, N.; Lu, X.; Zhang, W. *Chem. Lett.* **2007**, *36*, 1288.
(44) Jeevananda, T.; Lee, J.; Siddaramaiah, H. *Mater. Lett.* **2008**, *62*, 3995.
(45) Zhang, L.; Peng, H.; Zujovic, Z. D.; Kilmartin, P. A.; Travas-Sejdic, J. *Macromol. Chem. Phys.* **2007**, *208*, 1210.
(46) Zujovic, Z. D.; Zhang, L.; Bowmaker, G. A.; Kilmartin, P. A.; Travas-Sejdic, J. *Macromolecules* **2008**, *41*, 3125.
(47) Minami, H.; Okubo, M.; Murakami, K.; Hirano, S. *J. Polym. Sci., Part B: Polym. Phys.* **2000**, *38*, 4238.
(48) Okubo, M.; Fujii, S.; Minami, H. *Colloid Polym. Sci.* **2001**, *279*, 139.

2. Experimental Section

Reactants. Distilled aniline, ammonium persulfate, and *p*-toluenesulfonic acid were used as the starting reactants; all were obtained from Sigma Aldrich. (The role of the acid has been thought to be structurally directing[29] though this has recently been questioned.[20,24,26,33]) Milli-Q purified water was used to prepare a solution containing aniline and *p*-toluenesulfonic acid, with the resulting mixture refrigerated at 3 °C for 1 h. A separate solution containing ammonium persulfate was also prepared using Milli-Q water and refrigerated. These concentrations were twice as dilute as in some other studies,[13,17,20,24,25] to improve the precision of pH-stat control and to achieve a more gradual 20-h morphological evolution. The aforementioned solutions were then mixed together in an ice-bath-cooled pH-stat setup at 4 ± 1 °C, giving final concentrations of 0.133 M aniline, 0.067 M *p*-toluenesulfonic acid, and 0.133 M ammonium persulfate.

pH-stat. The pH-stat apparatus consisted of a Metrohm 836 Titrando base, 800 Dosino dosing unit, 804 Ti stand, stirrer, electrode, and software. The acidity was kept constant by automatic titration with 0.1 M sodium hydroxide. The stirrer ensures that the three aforementioned reagents and the added base are well-mixed. A typical pH-2-stat experiment is shown in Figure 1, with the corresponding titration curve showing the volume of sodium hydroxide added to keep the pH constant. Note the mirrored similarities between the profiles of the falling-pH curve and the titration curve of the pH-stat experiment. The lowest stirring speed and smallest stirrer available were used for the pH-stat setup: a propeller-type stirrer, 2 cm in diameter, spun at approximately 125 rpm. Before every experimental run the apparatus was calibrated using pH-buffer standards from LabServ. Since the reagent solution has an initial pH of approximately 7, it was necessary to lower pH at the beginning of the reaction to reach the targeted pH by adding 1 M sulfuric acid, which was chosen for its compatibility with the reaction (the ammonium persulfate oxidant produces sulfuric acid as well).

Once the reaction started, the pH and the volume of the base added were logged by the Metrohm software at 10-s intervals, and approximately 2 μL samples were manually pipetted out from the ongoing reaction for subsequent testing. The extracted samples were immediately centrifuged and repeatedly washed and were then vacuum-dried for 20 h. Previous studies have reported difficulties with pH electrodes in PANI solutions,[78] since the synthesis process will coat every available surface with a polymer layer. A coated electrode will affect the accuracy of pH readings, particularly for thicker coatings, which in turn are a function of initial reagent concentration. After the reactions finished, the PANI-coated electrode was tested against a known pH-buffer standard, and we also used a separate, uncoated Sartorius PB-11 pH meter to measure the final pH of the PANI solution. In both cases it was determined that the pH reading error of the used electrode was approximately ±0.3.

Characterization. A Philips XL30S field emission scanning electron microscope (SEM) and a JEOL TEM-2010 transmission electron microscope (TEM) were used to image the PANI morphology. SEM samples were mounted on aluminum studs using double-sided graphite tape and were then sputter-coated using platinum to improve conductivity and thereby alleviate charging artifacts. TEM samples were dispersed in ethanol by ultrasonication and then pipetted onto copper coated grids. Fourier transform infrared (FTIR) spectra were recorded with a PerkinElmer Spectrum 400 spectrometer in ATR mode using a Diamond/ZnSe crystal, at 4 cm^{-1} resolution and using four scans. The ultraviolet−visible spectroscopy (UV/vis) spectra were recorded with a Shimadzu UV-1700 spectrophotometer, at a 1 nm sampling interval, in single scan mode, with a 340.8 nm light source wavelength, on samples dispersed in Milli-Q purified water[79] by 30 s ultrasonication in an Elma Ultrasonic LC30H. The four-point conductivity measurements were done at room temperature using a Jandel RM2 test unit, on cylindrical pellets (1.5 cm diameter, 0.7 cm thickness) that were formed by applying 7 tons of pressure for 5 min using a vacuum press.

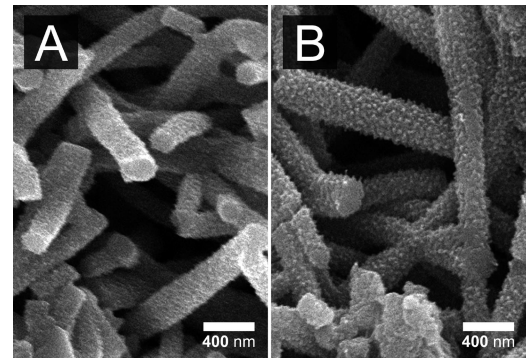

Figure 2. Comparison of conventional PANI nanotube synthesis (A) and stirred synthesis (B).

3. Results and Discussion

3.1. Control Experiment. A control experiment was first performed to determine whether switching from the conventional unstirred, sealed, refrigerated reaction pathway[18] to a stirred, open-beaker, ice-bath cooled pathway affects the formation of PANI nanotubes. In particular, reports from Huang and Kaner have shown that fast stirring can suppress secondary growth and generate high-purity nanofibers when PANI synthesis is carried out in strongly acidic 1 M HCl solution.[49] The control experiment thus compared a stirred, ice-bath cooled experiment with a nonstirred, refrigerated experiment, neither of which involved any pH-stat or pH-altering conditions. As Figure 2 shows, nanotubes were formed in both cases, with similar sizes, purity, and morphology, which we attribute to the negligible effect of our low stirring speed.

3.2. SEM Results. The chemical oxidation of PANI was carried out via six separate pH-stat experiments, and Figure 3 summarizes the variety of nanostructures formed. Their morphological evolution is shown as a function of time, with samples extracted during three distinct periods: the first 10 min, the first 2 h, and the last hours of the 20-h synthesis. As noted in the introduction, the oxidation of PANI gradually increases the acidity of the solution, from an initially neutral pH to a low final pH. Thus, the summary of the morphologies shown in Figure 3 covers the experimentally interesting acidity range encountered in most previous studies, giving our results a wide applicability as a potential "map" of the nanostructured products that self-assemble during aniline oxidation.

An immediately obvious implication of Figure 3 is the relatively well-separated occurrence of morphologies as a function of pH. Although some previous studies have been able to selectively produce a few of these morphology types,

(49) Huang, J.; Kaner, R. B. *Angew. Chem., Int. Ed.* **2004**, *43*, 5817.

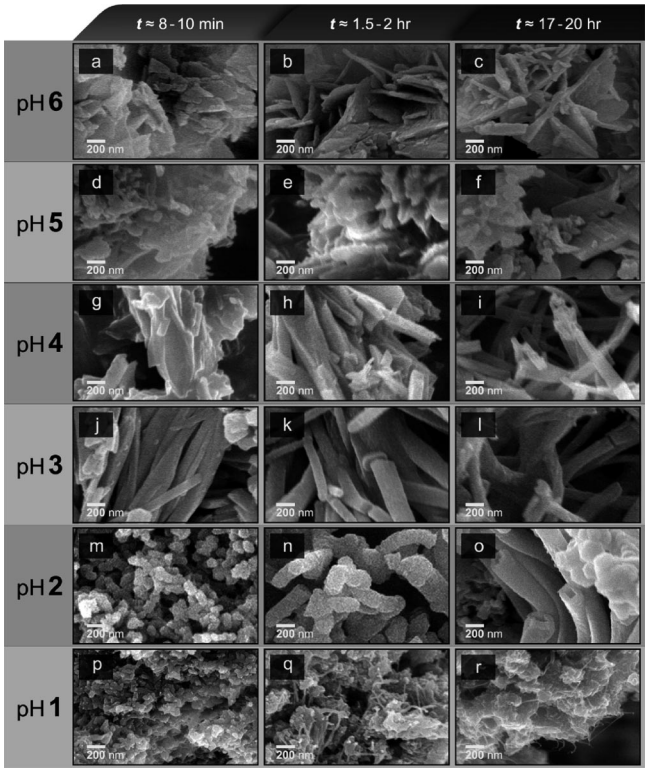

Figure 3. SEM images of six separate pH-stat experiments, each keeping the pH constant at 1, 2, 3, 4, 5, and 6, respectively. The morphological evolution is shown as a function of time. Images show the same magnification.

by varying reagent ratios,[50−52] time,[53] pH,[17] and even the type of polymerization,[54] we believe our pH-stat method is the first to isolate such a wide spectrum of morphologies with relatively good selectivity. This separation provides a clearer picture of why the final products of a typical falling-pH study are a mixture of nanofibers, nanotubes, nanoparticles, and nanoflakes and should help assign each type of morphology that is detected to a specific acidity region of the falling-pH reaction. Furthermore, this separation can provide a guide for the production of nanostructures of improved purity. This separation also allows for more accurate characterization (e.g., FTIR results, see Section 3.4), as materials previously characterized included a multitude of morphologies and structures produced at different pH values during the reaction.

More importantly, the results summarized in Figure 3 show a hitherto unexplored aspect of morphological evolution, demonstrating that even at the same pH the PANI nanostructures will progress as a function of time. In previous studies this passing of time and the increase of acidity happened simultaneously so that the effects of these two variables were convolved and inseparable. Using the pH-stat approach we report the separation of the two variables, showing that each has an individual effect on PANI nanostructure self-assembly. Taking the pH-4-stat experiment as

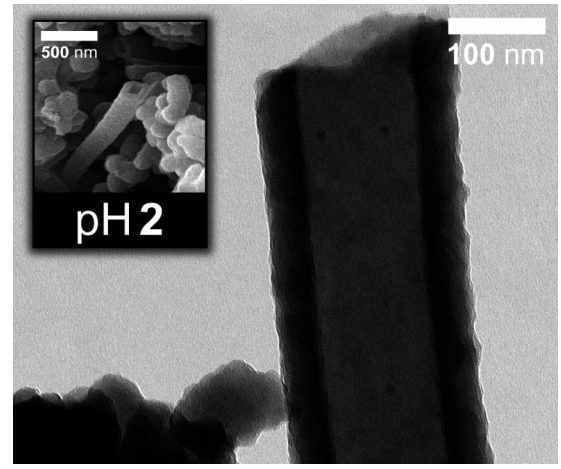

Figure 4. TEM image of the final product of pH-2-stat synthesis (with the corresponding SEM image shown in the inset).

an example, we see that the flat, ribbon-like structures present are larger and agglomerated during the first few minutes of the reaction, which gradually become finer in structure and better-separated after a few hours. This has important implications, since it is generally accepted that the initial higher-pH products will interact with the subsequent nanostructure formation at lower pH, with phenazine formation theory even suggesting that the rod or ribbon-like structures initially formed (here, at pH-4-stat) serve as the inner templates that seed nanotube formation.[25] Our results, which show that nanostucture size varies as a function of time even when pH is held constant, may be able to expand template-backed formation theories by suggesting a reason for the difference in feature sizes; that is, changing nanorod size may change the inner diameters of the resulting nanotubes. Depending on concentration, the kinetics of a reaction will be sped up or slowed down, which in turn may affect the size and type of intermediate nanorod structures formed. With reference to our pH-4-stat example, a high-concentration reaction may pass through the initial pH 4 stage around $t = 8-10$ min, with a large and highly agglomerated type of ribbons, while the slower kinetics of a lower concentration may allow for the pH 4 stage to evolve toward the finer-featured set of rods seen at $t = 17-20$ h.

Also novel is the formation of nanotubes and nanofibers in pH-stat conditions. That such morphologies can form at pH-2-stat and pH-3-stat conditions is surprising, since these constant-acidity syntheses bypass any prolonged upper-pH stage, and may thus prevent the formation of characteristic flake or ribbon-like structures that are sometimes credited as nanotube templates.[25] Since a detailed investigation of nanotube formation is a departure from the focus of this present study on mapping the variety of PANI morphologies using pH-stat, we will report our nanotube-specific studies in a subsequent communication.

3.3. TEM Results. Figures 4−6 are TEM images of selected final products, focusing on the nanotubes and nanoparticles formed at pH 2, the nanotubes and nanofibers formed at pH 3, and the nanorods and nanoribbons formed at pH 4, respectively. Figure 5 is important to demonstrate that the pH 3 products do contain hollow nanotubes, since this inner structure is not discernible from SEM imaging

(50) Amarnath, C. A.; Kim, J.; Kim, K.; Choi, J.; Sohn, D. *Polymer* **2008**, *49*, 432.
(51) Ding, S.; Mao, H.; Zhang, W. *J. Appl. Polym. Sci.* **2008**, *109*, 2842.
(52) Wang, X.; Liu, N.; Zhang, W. J. *Solid State Phenom.* **2007**, *121−123*, 429.
(53) Zhang, H.; Wang, J.; Zhou, Z.; Wang, Z.; Zhang, F.; Wang, S. *Macromol. Rapid Commun.* **2008**, *29*, 68.
(54) Anilkumar, P.; Jayakannan, M. *Macromolecules* **2008**, *41*, 7706.

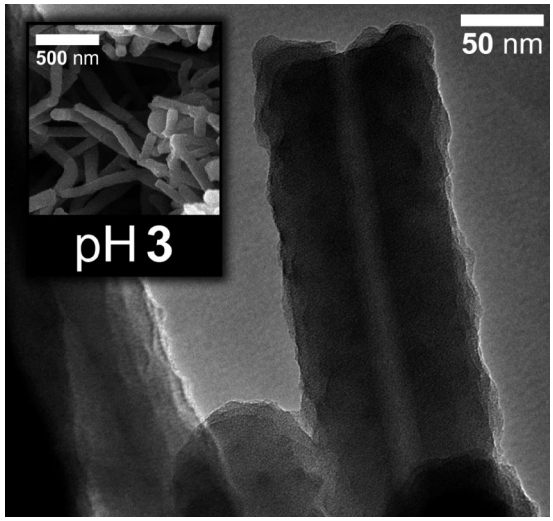

Figure 5. TEM image of the final product of pH-3-stat synthesis (with the corresponding SEM image shown in the inset).

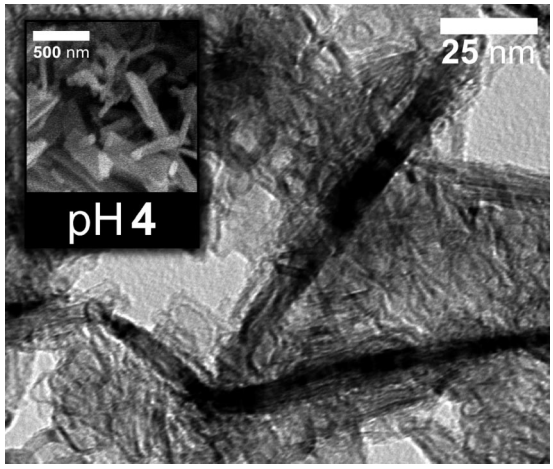

Figure 6. TEM image of the final product of pH-4-stat synthesis (with the corresponding SEM image shown in the inset).

alone. Although the pH 3 products are a mixture of nanotubes and nanofibers, the yield of these nanostructures is 80−90%, which contrasts the pH 2 yield of 10−20% nanotubes (the remaining are granular particles, as seen in the lower left corner of Figure 4).

It is interesting to contrast the surface texture of the nanotubes and nanofibers that are formed in pH-2-stat and pH-3-stat conditions with the much finer, almost crystalline-like[55] texture of the short nanorods formed in pH-4-stat conditions, which are illustrated in Figure 6. Taking into account only the pH-2-stat and pH-3-stat nanotubes and nanofibers, one could plausibly make an argument for a self-assembly theory based on small micelles,[10,26−34] but once the pH-4-stat smooth nanorods are also considered, it seems that an additional mechanism may be required. Indeed, Gao et al. have proposed that this fine alignment seen in oligomers is due to the flat stacking of phenazine-like structures, achieved via $\pi-\pi$ interactions between the aligned layers

(55) Mazerolles, L.; Folch, S.; Colomban, P. *Macromolecules* **1999**, *32*, 8504.

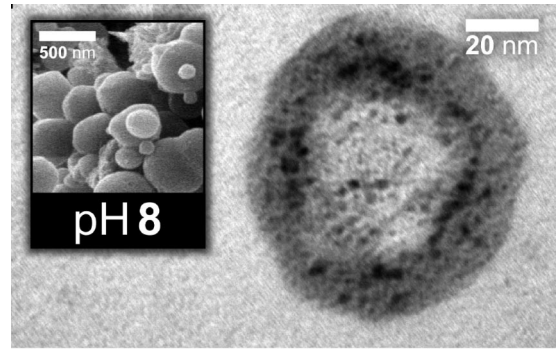

Figure 7. TEM image of the final product of pH-8-stat synthesis (with the corresponding SEM image shown in the inset).

of the constituent rings of phenazine.[56] The authors go further to suggest a nanotube self-assembly scheme where the high-pH oligomers serve as a template for lower-pH nucleation and that as the pH falls further still, the oligomer template dissolves, leaving behind a hollow tube. However, our nanotubes form at constant pH-2-stat and pH-3-stat conditions, which has two key implications: first, the pH level should be too low for oligomer template formation,[20] and second, there is no lowering of pH that would allow the oligomer template to dissolve.[56]

It has been proposed that the limited miscibility of neutral aniline leads to the formation of a separate droplet phase, with oxidation then progressing at the surface of the droplet and leading to the growth of nanospheres and microspheres.[17] Indeed, at even higher pH values we produced the spherical morphologies shown in Figure 7, with some of the spheres apparently hollow and others possibly filled with aniline,[17] although varying reagent ratios have also been proposed as a reason for this difference.[52] This makes for an interesting point of comparison with previous aniline microsphere studies. Stejskal et al. reported the production of these microspheres and nanospheres in a synthesis carried out in alkaline 0.2 M ammonium hydroxide medium, which had its pH fall from 10 to 3 during the course of a 2-h reaction.[17] Using the pH-stat approach, we found the spherical morphology being produced in the pH 8 region, consistent with and perhaps clarifying that earlier study. However, as Venacio et al. have shown, varying the synthesis conditions can allow for the production of microspheres at even lower pH. The authors used a relatively dilute 0.01 M concentration of aniline, ammonium persulfate, and hydrochloric acid as their starting reagents, resulting in a falling-pH reaction that began at pH 4, producing microspheres between pH 4 and 3 in the first 22 h, and eventually falling to pH 2 after a few days, a region in which fibrilar and granular morphologies were observed.[57] Venacio et al. propose that at these higher pH values "azanes" with an N−N backbone are formed rather than true PANI, with this difference in the chemical structure of the chains accounting for the change in morphology. Yet another approach to microsphere synthesis has been to vary the ratio of acid to aniline, which Zhang and Wan have

(56) Gao, C.; Guan, M.; Li, H.; Sun, J.; Xu, Z. *Adv. Funct. Mater.* **2008**, submitted.
(57) Venancio, E. C.; Wang, P.-C.; MacDiarmid, A. G. *Synth. Met.* **2006**, *156*, 357.

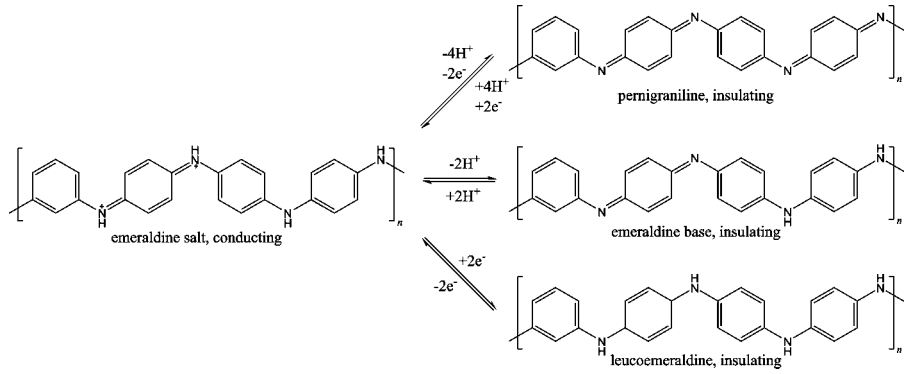

Figure 8. Various states of PANI: emeraldine salt, pernigraniline, emeraldine base, and leucoemeraldine.

shown to change the final morphology of self-assembly from nanotubes to microspheres.[27] Although no pH values were recorded during that study, the reagents used, aniline, ammonium persulfate, and doping acid, are typical of a falling-pH synthesis. The authors proposed that hydrogen bonding between the hydroxyl group of the acid and the amine group of the PANI backbone is the driving force behind microsphere self-assembly, pointing out that once magnetic stirring was added, it disrupted the hydrogen bonding and prevented the formation of the spherical morphology. (Interestingly, the spherical morphology of our pH-stat study was achieved under stirred conditions.) It is also worthwhile to note that although our and the three aforementioned microsphere studies[17,27,57] used somewhat different approaches to synthesis conditions, the overall trend present in all was the same transition between morphologies, from spherical to fibrilar, as the pH or dopant ratio parameters were changed.

3.4. FTIR Results. Before presenting the FTIR spectra, it is worth reviewing the structural forms of PANI. The simplest type of PANI can be thought of as a chain of *p*-phenyleneimine repeated units, altogether referred to as leucoemeraldine form of aniline,[58] shown in Figure 8. Leucoemeraldine is insulating, but its oxidation will lead to the formation of iminoquinones in the polymer structure. Partial oxidation creates the emeraldine base form, whose poor conductivity of $\sigma < 10^{-10}$ S cm^{-1} can be improved by 10 orders of magnitude when doped, yielding $\sigma > 1$ S cm^{-1}. These structures are shown in Figure 8. Further oxidation yields the pernigraniline form, which is insulating, and is also shown in Figure 8. This general scheme is particularly relevant for our study, since the strict control of pH levels will determine the activity of H^+ and H_3O^+ ions in the solution, thus affecting the structure of the PANI chains themselves.[24,59] The importance of pH has been shown by the pioneering cyclic voltammetry studies on PANI films, where it was observed that raising pH decreases electrochemical activity, with the films becoming completely insulating for pH levels above 3 or 4.[60] Recent studies on PANI nanostructures and microstructures have similarly shown that when the pH is kept high, starting at 10 and

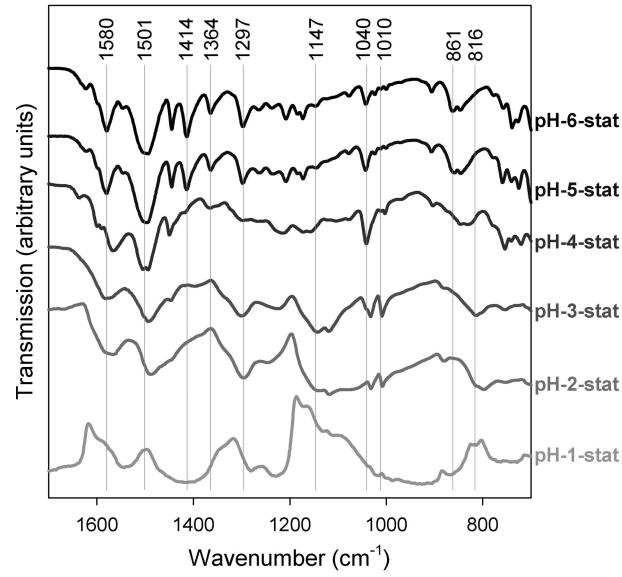

Figure 9. FTIR transmission spectra of the final products (after 20 h of reaction time) of six separate pH-stat experiments, each keeping the pH constant at 1, 2, 3, 4, 5, and 6, respectively. These spectra correspond to the last column of SEM images in Figure 3 and to the TEM images shown in Figures 4−6.

finishing at 3, the resulting products are insulating, with a conductivity below 10^{-10} S cm^{-1}.[17]

The FTIR spectra of the final 20-h products of various pH-stat reactions are shown in Figure 9. The 1580 cm^{-1} band is characteristic of quinone diimine ring-stretching deformation, while the 1501 cm^{-1} band indicates benzenoid diamine ring stretching.[61] The relative intensities of the two hint at the structure of the polymer backbone, with the higher intensity of the 1501 cm^{-1} band placing the structure closer to the emeraldine rather than leucoemeraldine form of PANI. (Pure leucoemeraldine would be expected to have practically no 1580 cm^{-1} quinoid band, while for pure emeraldine the intensities of the two bands should be similar, albeit favoring the 1501 cm^{-1} benzenoid band.[61,62] This is only a qualitative measure, however, as the quinoid to benzenoid band ratio of emeraldine can vary significantly with synthesis conditions and scales nonlinearly with the extent of oxidation.[63]) More

(58) Karyakin, A. A.; Vuki, M.; Lukachova, L. V.; Karyakina, E. E.; Orlov, A. V.; Karpachova, G. P.; Wang, J. *Anal. Chem.* **1999**, *71*, 2534.
(59) Ge, C.; Armstrong, N. R.; Saavedra, S. S. *Anal. Chem.* **2007**, *79*, 1401.
(60) Kobayashi, T.; Yoneyama, H.; Tamura, H. *J. Electroanal. Chem.* **1984**, *177*, 281.
(61) Kang, E. T.; Neoh, K. G.; Tan, K. L. *Prog. Polym. Sci.* **1998**, *23*, 277.
(62) Quillard, S.; Louarn, G.; Lefrant, S.; MacDiarmid, A. G. *Phys. Rev. B* **1994**, *50*, 12496.
(63) Asturias, G. E.; Macdiarmid, A. G.; Mccall, R. P.; Epstein, A. J. *Synth. Met.* **1989**, *29*, E157.

importantly, as the pH-stat value is lowered, a clear decrease of the wavenumbers of the quinone and benzenoid bands is observed. Taking the quinone rings as an example, we see in Figure 9 that the 1580 cm^{-1} band at pH-6-stat shifts down to 1545 cm^{-1} for the pH-1-stat experiment. This red-shift is due to the protonation of the PANI base[64] and indicates that the doping level and conductivity of the PANI nanostructures is increasing as the pH-stat level is decreased. Further support comes from the 1147 cm^{-1} band, which has been assigned to either $-NH^+$ stretching modes of the doped state[18] or to the high degree of electron delocalization of that doped state.[65] This doped state band is not present at the higher pH-stat levels, appearing only in the samples prepared at pH 3, 2, and 1, which will be explored in further detail in the UV/vis section of this study.

Phenazine-like units have been proposed by Stejskal et al. as the key starting template for the self-assembly of PANI nanotubes[20,23,25,35,36] and as most likely to be formed at pH higher than 4.[20] Multiple bands have been suggested as indicative of phenazine units:[17,20] 1625 cm^{-1} for the C═C stretching vibration, 1416 cm^{-1} for symmetric ring stretching, and 1208 cm^{-1}, a contribution to 1145 cm^{-1}, 1136 cm^{-1}, and 1108 cm^{-1}. Since ortho-coupling is the precursor to phenazine unit formation, FTIR spectra of the two are difficult to separate, and the 1630 cm^{-1}, 1445 cm^{-1}, and 1416 cm^{-1} bands have been attributed to both.[17] This latter band, here present at 1414 cm^{-1}, is the strongest of these phenazine-like features, and its presence at the pH-5-stat and 6 levels diminishes greatly as the acidity increases, disappearing in the pH-2-stat product. This is explained by the 4.6 pK_a value of aniline, which defines a threshold below which the equilibrium shifts from neutral aniline toward the protonated anilinium cation form.[17] Unlike neutral aniline, which yields a mixture of ortho- and para-coupling, the anilinium cation cannot be easily oxidized and instead propagates onto existing chains in para-coupled positions. This preference for para-coupling in turn diminishes the occurrence of the ortho-coupled structures, preventing the formation of phenazine units via the oxidation of 1,2-disubstituted or 1,2,4-trisubstituted ortho-coupled ring structures. Further reinforcing the trend toward para-coupling are the relative intensities of the 861 cm^{-1} and 816 cm^{-1} bands: as the pH-stat level is decreased, there is a clear shift from ortho-coupling at 861 cm^{-1} toward para-coupling at 816 cm^{-1}, consistent with the aforementioned increase in para-coupling expected due to the low-pH presence of anilinium cations. A related structure to phenazine-like units is the quinuclidine-like rigid system based on a symmetrically three-substituted nitrogen atom, which has been associated with the 1448 cm^{-1} band,[66] although this band has also been attributed to a more general mix of C−C stretching and C−H and C−N bending observed in aromatic oligomers.[67]

Other features of the spectra include the 1364 cm^{-1} and 1297 cm^{-1} bands corresponding to C−N stretching in the proximity of quinoid rings, with the first of these bands due to benzenoid−*trans*-quinoid−benzenoid complexes and the second due to benzenoid−*cis*-quinoid−benzenoid, quinoid−benzenoid−benzenoid, and benzenoid−benzenoid−quinoid complexes.[61] Previous studies have reported that PANI synthesized at low pH values of 1 or 2 will have stronger C−N stretching bands than synthesis that finishes at a weaker acidity value of approximately pH 4,[17] which is consistent with the pH-stat results presented in Figure 9. The most important trend here is the decrease in intensity of the 1364 cm^{-1} band with falling pH, culminating in its complete disappearance at the lower pH-stat levels. This is due to the acid protonation of the PANI emeraldine base[61,68] so that the disappearance of the 1364 cm^{-1} band correlates to an increase in conductivity (see next section) and at the same time also corresponds to a morphology transition from ribbons to nanofibers and nanotubes.

Two FTIR vibrational frequencies at 1070 cm^{-1} and 1040 cm^{-1} have been associated with aryl-S groups, as a result of aromatic ring vibration with C−S stretching characteristics.[69] In our spectra, such vibrational frequencies are found in the pH-2-stat and pH-3-stat experiments, but although the 30 cm^{-1} spacing between them remains, the absolute values are shifted to 1040 cm^{-1} and 1010 cm^{-1}. The 1040 cm^{-1} band is also present in all of the pH-stat experiments, with its intensity increasing with higher pH. This band has also been assigned to sulfonate SO_3^- groups, although it is unclear if this due to the integration of sulfur into the polymer backbone[20] or simply the presence of hydrogen sulfate counterions.[18] Trchova et al. actually proposed the 1040 cm^{-1} band to be characteristic of the S═O stretching vibration mode, with the aniline monomers and oligomers found at pH 4 and higher being particularly prone to the eletrophilic attack of sulfonation, much more so than the anilinium cations that are present at lower pH.[20] This would explain why the sulfonate peaks in Figure 9 increase in intensity at higher pH. It is also likely that the incorporation of a sulfate group will have a steric effect on the conformation of the PANI chain,[70] deforming its planarity and thus diminishing conjugation[20] and reducing the overall conductivity.[71] This underscores the potential application of pH-stat methods to the separation of highly sulfonated, poorly conducting products formed at higher pH from the nanotubes and nanofibers that are formed in pH-2-stat and pH-3-stat conditions.

In addition to Figure 9, we also investigated how the FTIR spectra evolve as a function of synthesis time. This was done for all six pH-stat experiments, but due to space considerations two of these evolutions are presented in Figure 10. The spectra remain largely unchanged as a function of time, with the notable exceptions being an increase in the sulfonation bands as the reaction progresses, which previous studies have correlated with a decrease in conductivity,[70] and the benzenoid to quinone peak ratio increases, suggesting a

(64) Stejskal, J.; Trchova, M.; Blinova, N. V.; Konyushenko, E. N.; Reynaud, S.; Prokes, J. *Polymer* **2008**, *49*, 180.
(65) Neoh, K. G.; Kang, E. T.; Tan, K. T. *Polymer* **1993**, *34*, 3921.
(66) Langer, J. J.; Golczak, S. *Polym. Degrad. Stab.* **2007**, *92*, 330.
(67) Yadav, J. B.; Puri, R. K.; Puri, V. *Appl. Surf. Sci.* **2007**, *253*, 8474.
(68) Kang, E. T.; Neoh, K. G.; Tan, T. C.; Khor, S. H.; Tan, K. L. *Macromolecules* **1990**, *23*, 2918.
(69) Wei, X.-L.; Wang, Y. Z.; Long, S. M.; Bobeczko, C.; Epstein, A. J. *J. Am. Chem. Soc.* **1996**, *118*, 2545.
(70) Sahin, Y.; Pekmez, K.; Yildiz, A. *Synth. Met.* **2002**, *129*, 107.
(71) Stejskal, J.; Gilbert, R. G. *Pure Appl. Chem.* **2002**, *74*, 857.

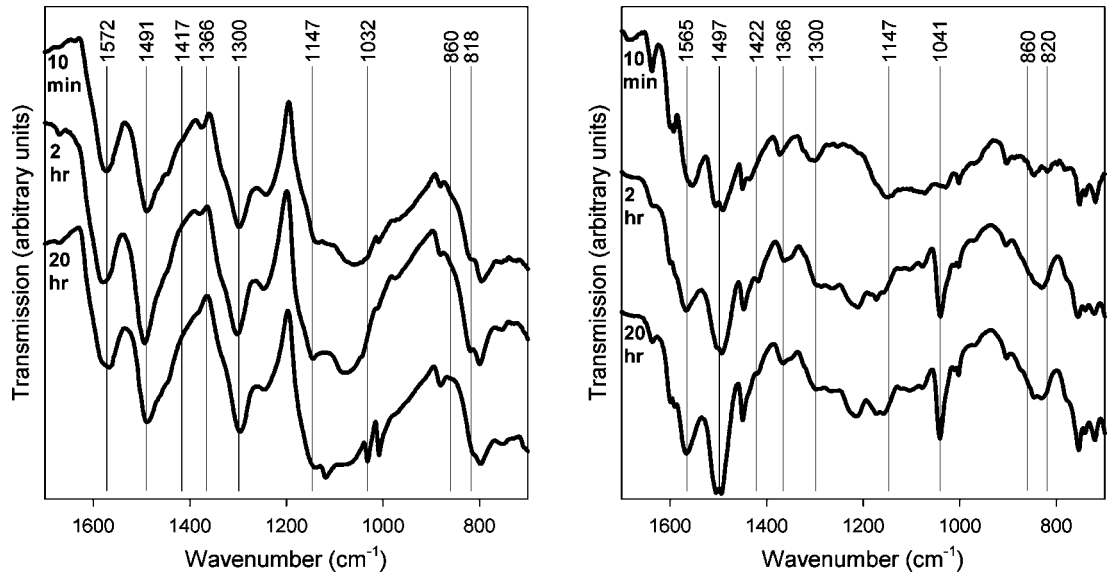

Figure 10. FTIR transmission spectra of pH-2-stat (left) and pH-4-stat (right) as a function of reaction time.

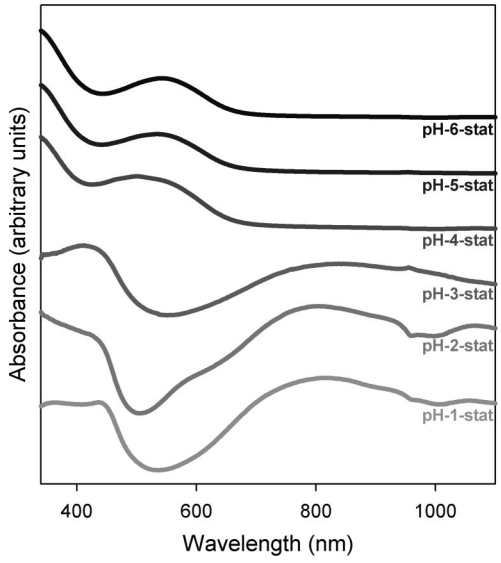

Figure 11. UV/vis spectra of the final 20 h pH-stat formation products, after postsynthesis redoping in excess H_2SO_4.

decrease in the extent of oxidation, perhaps as a result of ammonium persulfate oxidant depletion as the reaction finishes. The fairly consistent 1422 cm^{-1} phenazine band intensity of the product obtained at pH-4-stat, as well as an approximately constant ortho-coupling to para-coupling ratio (i.e., the 860 cm^{-1} to 820 cm^{-1} band ratio), are also typical of the pH-stat time evolutions. Specifically, to take an example not illustrated in Figure 10, the pH-6-stat FTIR spectra show ortho-coupling and strong phenazine presence at all times, and the pH-2-stat FTIR spectra are para-coupled and have little phenazine presence, also at all times, suggesting that these aspects of the PANI structure are more pH-determined and not affected by the passing of time when the pH is held constant.

3.5. UV/Vis and Conductivity Results. Figure 11 shows the UV/vis spectra of the final products of the pH-stat syntheses. The wide "tail" above the 800 nm wavelength is due to delocalized polaron transitions that are characteristic of conducting PANI.[72] Its presence in pH-1-stat products is expected, since it is well-known that PANI synthesized in a strongly acidic 1 M HCl medium yields a conductive polymer.[73] It is interesting that this delocalized polaron tail remains for the pH-2-stat and pH-3-stat synthesis products, corresponding to a morphology change from exclusively nanoparticles to nanotubes and nanofibers. The relative height of the 800 nm polaron tail does diminish somewhat for the products obtained at pH-3-stat, suggesting that while the nanotube and nanofiber samples are somewhat conductive, they are less so than the products formed at lower pH.

This was confirmed by conductivity measurements, where four-point probing of pelletized pH-2-stat products measured a conductivity of 1.1×10^{-1} S cm^{-1}, three orders of magnitude higher than the 1.0×10^{-4} S cm^{-1} conductivity of the pH-3-stat products. The conductivity of the pH-1-stat product was higher still, with a value of 1.6 S cm^{-1}. Meanwhile, the structures formed at more neutral pH, such as pH-4-stat and above, were found to be completely insulating, with conductivities on the order of 10^{-10} S cm^{-1}, consistent with previous reports.[17] As a control experiment, a pellet made out of PANI was also synthesized via conventional falling-pH oxidation, a pathway that includes structures generated at a variety of acidities, from pH 7 to pH 1. Since over 90% of the 20 h of reaction time of the falling-pH synthesis was at acidity lower than pH 1, one may expect that the conductivity of the resulting products would be higher than those products obtained by pH-2-stat synthesis. However, the mixture of structures obtained by falling-pH was found to have a conductivity value of only 4.9×10^{-2} S cm^{-1}, underscoring the advantage of the pH-stat synthesis method: it avoids the production of poorly conducting, phenazine-like products that are formed during the initial, higher-pH stages of conventional chemical oxidation. Incidentally these bulk conductivity values should be only

(72) Liu, W.; Kumar, J.; Tripathy, S.; Senecal, K. J.; Samuelson, L. *J. Am. Chem. Soc.* **1999**, *121*, 71.
(73) Ray, A.; Astarias, G. E.; Kershner, D. L.; Richter, A. F.; MacDiarmid, A. G.; Epstein, A. *Synth. Met.* **1989**, *29*, E141.

taken as relative comparisons between samples, not as absolute values, since contact resistance between nanotubes in compressed pellets decreases the conductivity by a factor of approximately 10^4 times when compared to an individually probed nanotube.[32]

The UV/vis spectra of the products obtained at pH-4-stat and higher show a complete disappearance of the delocalized polaron transition band. However, for the as-synthesized pH-stat products two separate effects may influence the presence of delocalized polarons: first, the type of the PANI structure (e.g., para-linked chains versus phenazine-like units), and second, the extent of protonation-induced doping. Since the different pH levels will affect the SO_4^{2-} to HSO_4^- counterion equilibrium that is present, the prevalence of doping ions will differ between the pH-stat syntheses. To test for this, the pH-stat synthesis products were doped postsynthesis, with excess sulfuric acid. Since this treatment did not alter the UV/vis spectra of the products, we attribute the failure of the pH-4-stat to pH-6-stat samples to give rise to a polaron transition band to structural defects and not a lack of doping. (The same holds for FTIR: when pH-6-stat products were doped postsynthesis, the spectral features did not change significantly.) As discussed in the previous section, these structural defects that are present at higher pH-stat levels may include ortho-linking, phenazine-like units, or deformed planarity due to sulfonation. It is also worth noting that the FTIR results shown in Figure 9 and the UV/vis results of Figure 11 are consistent, since the strong doped-state FTIR band present at approximately 1147 cm^{-1} displays the same trends as the strong delocalized-polaron UV/vis band at 800 nm: they are both the most prominent for products formed at pH-1-stat and pH-2-stat, diminishing but still present for products formed at pH-3-stat, and then disappear for products formed at pH-4-stat to pH-6-stat.

The other UV/vis features in pH-1-stat, pH-2-stat, and pH-3-stat products are at 360 nm ($\pi \rightarrow \pi^*$ band transition), 440 nm (polaron $\rightarrow \pi^*$ band transition), and 780 nm ($\pi \rightarrow$ polaron band transition), consistent with the theoretically described model of protonated emeraldine PANI[74] as well as experimental results from falling-pH method conducting PANI nanotubes[33] and conventional 1 M HCl method granular PANI.[75] None of these bands are apparent for the higher pH-stat products, which instead display features at approximately 550 and 340 nm, which are typically assigned to the higher-pH, insulating forms of PANI[76] and that Venacio et al. have even assigned to "azanes", a N−N backbone polymeric product that forms during the higher-pH stages of a falling pH PANI chemical oxidation.[57]

4. Conclusions

We have used pH-stat synthesis to pursue a two-pronged approach to PANI nanostructure morphology, by presenting newly observed phenomena and by isolating, organizing, and characterizing already known structures. The newly observed phenomena include the time-dependent evolution of morphology at constant pH, an increase in sulfonation and decrease in oxidation as the reaction progresses (even when the pH is kept constant), and the formation of nanotubes and nanofibers in pH-2-stat and pH-3-stat conditions. The investigation of known structures was done using SEM, TEM, FTIR, UV/vis, and four-point conductivity measurements, systematically charting nanostructure evolution in a way that separates structure, morphology, pH, and time effects.

Future work will look to apply the pH-stat approach to further structure and property investigations such as nuclear magnetic resonance, electron paramagnetic resonance, elemental analysis, and X-ray spectroscopy, which are bulk analysis methods that depend on sample homogeneity. With the sole exception of the four-point probing of an individual nanotube,[32,77] previous studies have actually analyzed a mixture of different structures and morphologies, giving a convolution of spectra and other data. For example, an investigation of a sample extracted at pH 3 during a typical falling-pH synthesis will actually include samples from pH 3, pH 4, pH 5, and pH 6, making for uncertain analysis results, with properties attributed to nanotubes possibly being due to a mixture of nanotubes, nanoribbons, and nanoflakes. This is where a pH-stat approach will be useful, isolating different stages of the synthesis process as illustrated in Figure 3. We will also investigate why nanotubes can form in pH-2-stat and pH-3-stat conditions, despite the apparent lack of non-PANI oligomer templates that have been previously described as a prerequisite for nanotube formation.

Acknowledgment. The authors thank the University of Auckland for Postdoctoral Fellowship funding.

CM803447A

(74) Xia, Y.; Wiesinger, J. M.; MacDiarmid, A. G.; Epstein, A. J. *Chem. Mater.* **1995**, *7*, 443.
(75) Angelopoulos, M.; Dipietro, R.; Zheng, W. G.; MacDiamid, A. G.; Epstein, A. J. *Synth. Met.* **1997**, *1997*, 35.
(76) Stejskal, J.; Kratochvil, P.; Radhakrishnan, N. *Synth. Met.* **1993**, *61*, 225.
(77) Long, Y.; Zhang, L.; Ma, Y.; Chen, Z.; Wang, N.; Zhang, Z.; Wan, M. *Macromol. Rapid Commun.* **2003**, *24*, 938.
(78) Stejskal, J.; Spirkova, M.; Kratochvil, P. *Acta Polym.* **1994**, *45*, 385.
(79) Chakraborty, M.; Mukherjee, D. C.; Mandal, B. M. *Langmuir* **2000**, *16*, 2482.